

This manuscript has been authored by UT-Battelle, LLC under Contract No. DE-AC05-00OR22725 with the U.S. Department of Energy. The United States Government retains and the publisher, by accepting the article for publication, acknowledges that the United States Government retains a non-exclusive, paid-up, irrevocable, world-wide license to publish or reproduce the published form of this manuscript, or allow others to do so, for United States Government purposes. The Department of Energy will provide public access to these results of federally sponsored research in accordance with the DOE Public Access Plan(<http://energy.gov/downloads/doe-public-access-plan>).

Spin-lattice coupling mediated multiferroicity in $(\text{ND}_4)_2\text{FeCl}_5\cdot\text{D}_2\text{O}$

W. Tian,^{1,*} Huibo Cao,¹ Jincheng Wang,¹ Feng Ye,¹ M. Matsuda,¹ J.-Q. Yan,^{2,3} Yaohua Liu,¹ V. O. Garlea,¹ B. C. Chakoumakos,¹ B. C. Sales,² Randy S. Fishman,² and J. A. Fernandez-Baca^{1,4}

¹Quantum Condensed Matter Division, Oak Ridge National Laboratory, Oak Ridge, Tennessee 37831, USA

²Materials Science and Technology Division, Oak Ridge National Laboratory, Oak Ridge, Tennessee 37831, USA

³Department of Materials Science and Engineering,

University of Tennessee, Knoxville, Tennessee 37996, USA

⁴Department of Physics and Astronomy, The University of Tennessee, Knoxville, Tennessee 37996, USA

(Dated: September 17, 2021)

We report a neutron diffraction study of the multiferroic mechanism in $(\text{ND}_4)_2\text{FeCl}_5\cdot\text{D}_2\text{O}$, a molecular compound that exhibits magnetically induced ferroelectricity. This material exhibits two successive magnetic transitions on cooling: a long-range order transition to an incommensurate (IC) collinear sinusoidal spin state at $T_N=7.3$ K, followed by a second transition to an IC cycloidal spin state at $T_{FE}=6.8$ K, the later of which is accompanied by spontaneous ferroelectric polarization. The cycloid structure is strongly distorted by spin-lattice coupling as evidenced by the observations of both odd and even higher-order harmonics associated with the cycloid wave vector, and a weak commensurate phase that coexists with the IC phase. The appearance of the 2nd-order harmonic coincides with the onset of the electric polarization, thereby providing unambiguous evidence that the induced electric polarization is mediated by the spin-lattice interaction. Our results for this system, in which the orbital angular momentum is expected to be quenched, are remarkably similar to those of the prototypical TbMnO_3 , in which the magnetoelectric effect is attributed to spin-orbit coupling.

PACS numbers: 77.80.-e, 75.25.-j, 61.50.Ks, 75.30.Kz

“Improper multiferroics” (also referred as type-II magnetic multiferroics) are a unique group of materials that exhibit direct coupling between magnetism and electric polarization^{1,2}. In these magnetically induced multiferroics, the magnetoelectric (ME) effect is strong and the onset of ferroelectricity arises directly from magnetic order that breaks spatial inversion symmetry. Due to the strong ME effect, there has been enormous interest in these materials motivated by their potential applications in novel multifunctional devices. However, natural single-phase magnetically driven multiferroics are rare, only a few transition-metal oxides such as TbMnO_3 ³⁻⁹, MnWO_4 ¹⁰, $\text{Ni}_3\text{V}_2\text{O}_8$ ¹¹, CuO ¹², LiCuVO_4 ¹³, and CaCoMnO_3 ¹⁴ are currently known to exhibit such effect. It is thus of great interest to discover and investigate new materials that will shed light on the underlying multiferroic mechanism. Recent efforts to search for new multiferroics have been extended to molecular compounds and metal-organic framework materials (MOFs)¹⁵. In particular, several ionic salts containing NH_4 have been reported to exhibit ferroelectricity¹⁶ and the incorporation of NH_4 has been used as a strategy to search for new multiferroics¹⁷⁻¹⁹. In this paper, we report a neutron diffraction study of the multiferroic mechanism in $(\text{NH}_4)_2\text{FeCl}_5\cdot\text{H}_2\text{O}$. Using both polarized and unpolarized neutrons, we show that the induced ferroelectricity in $(\text{NH}_4)_2\text{FeCl}_5\cdot\text{H}_2\text{O}$ is mediated via spin-lattice coupling mechanism strikingly similar to TbMnO_3 .

$(\text{NH}_4)_2\text{FeCl}_5\cdot\text{H}_2\text{O}$ belongs to the erythrosiderite-type compounds $A_2[\text{FeX}_5\cdot\text{H}_2\text{O}]$, where A is an alkali metal or ammonium, and X is a halide ion²⁰⁻²³. It crystallizes in an orthorhombic structure at room temperature (space

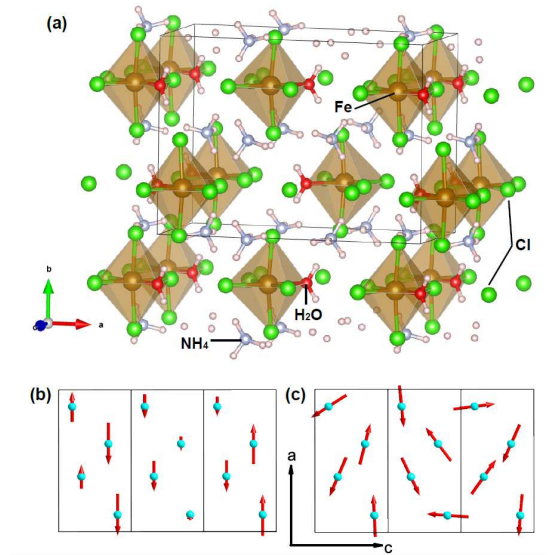


FIG. 1. (Color online) (a) Crystal structure of $(\text{NH}_4)_2\text{FeCl}_5\cdot\text{H}_2\text{O}$. (b) IC collinear sinusoidal spin structure at 7 K in the paraelectric phase; (c) IC cycloidal-spiral spin structure at 4 K in the ferroelectric phase, as viewed along the b -axis (three unit cells along c -axis are plotted). Only magnetic Fe ions are shown in (b) and (c) for the purpose of clarity.

group $Pnma$) with a crystal structure consisting of distorted $[\text{FeCl}_5\cdot\text{H}_2\text{O}]^{2-}$ octahedra linked by a network of hydrogen bonds²⁴ as illustrated in Fig. 1 (a). The orbital angular momentum of the magnetic Fe^{3+} ($3d^5$, high spin state) ion is expected to be completely quenched. The

magnetic interactions in these materials are mediated via multiple superexchange pathways, such as Fe-Cl \cdots Cl-Fe, Fe-O \cdots Cl-Fe, and Fe-O-H \cdots Cl-Fe involving hydrogen bonds, suggesting the presence of magnetic frustration in the system²³. (NH₄)₂FeCl₅·H₂O²⁴ is the only compound that exhibits spontaneous electric polarization in the A₂[FeX₅·H₂O] series. In sharp contrast to other isostructural counterparts, such as (K, Rb)₂FeCl₅·H₂O which undergo a single magnetic transition adopting a collinear antiferromagnetic (AFM) spin structure with moments along the *a*-axis²² and have no spontaneous electric polarization, (NH₄)₂FeCl₅·H₂O exhibits two magnetic transitions at $T_N \sim 7.3$ K and $T_{FE} \sim 6.8$ K, respectively. A disorder-order transition also occurs at $T_s \sim 79$ K associated with the motion of the NH₄ group²⁵. Unlike other NH₄ contained materials investigated so far^{17–19} where ferroelectricity is induced via the disorder-order transition at high temperature decoupled with the low temperature magnetic order, which is characteristic of the so called type-I “proper multiferroics”^{1,2}, (NH₄)₂FeCl₅·H₂O remains paraelectric below 79 K and spontaneous electric polarization only appears below T_{FE} . Consequently, it is crucial to know the magnetic structure and microscopic interactions to unveil the underlying mechanism responsible for the multiferroic properties in this compound. However, the determination of the full magnetic structure has been hampered due to the large amount of hydrogen atoms (40 H atoms per unit cell) in (NH₄)₂FeCl₅·H₂O.

We have grown deuterated (ND₄)₂FeCl₅·D₂O single crystals suitable for neutron scattering by solution method using starting materials (DCl, FeCl₃, and ND₄Cl) similar to that reported in Ref. 24. The saturated solution was sealed and kept at 38°C using a sample environment chamber to allow slow evaporation. Large deuterated crystals were obtained and later characterized by magnetic susceptibility and specific heat measurements. No significant deuteration-induced effects were observed since specific heat data indicates no transition temperature changes compared to the hydrogenated samples^{21,24}. Elastic neutron scattering experiments were carried out using the HB1, HB1A triple-axis spectrometer (TAS), and HB3A Four-Circle Diffractometer located at the High Flux Isotope Reactor (HFIR), and the Elastic Diffuse Scattering Spectrometer (CORELLI) at the Spallation Neutron Source (SNS) at Oak Ridge National Laboratory (ORNL). The magnetic structures at 4 K and 7 K were determined by refining the data collected at HB3A. HB1A and CORELLI were used to investigate the temperature and *q* dependence of the observed higher-order harmonics associated with the cycloid order. The nature of the higher-order harmonics were further clarified by polarized neutron experiments using the HB1 polarized TAS. The polarization of the incident beam and the polarization analysis of the scattered beam were produced by Heusler crystals, and a Mezei spin flipper was used for reversing the neutron polarization vector.

Neutron data show that (ND₄)₂FeCl₅·D₂O undergoes an incommensurate (IC) AFM long range order (LRO)

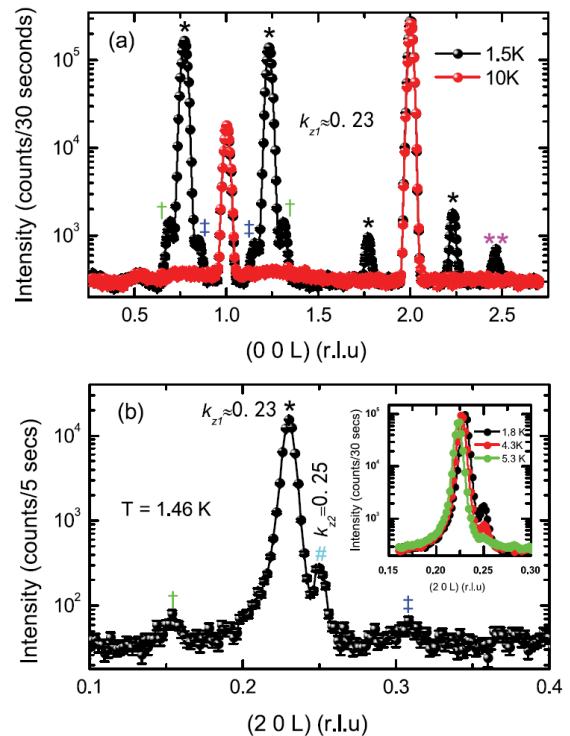


FIG. 2. (Color online) L-scans along both (0 0 L) and (2 0 L) with the intensity plotted on a logarithmic scale. (a) (0 0 L) scan measured at 1.5 K and 10 K. The primary IC satellites (0 0 $n \pm k_{z1}$), and the 2nd (0 0 $n \pm 2k_{z1}$), 3rd (0 0 $n \pm 3k_{z1}$), 5th order (0 0 $n \pm 5k_{z1}$) harmonic peaks are marked by * (black), ** (pink), † (green) and ‡ (blue), respectively (*n* is an integer). (b) (2 0 L) scan measured at 1.5 K reveals the coexistence of IC and commensurate phases. The primary IC satellites (2 0 $n \pm k_{z1}$), 3rd (2 0 $n \pm 3k_{z1}$), 5th-order (2 0 $n \pm 5k_{z1}$) harmonic peaks and the commensurate peak (2 0 $n \pm k_{z2}$) are marked by * (black), † (green), ‡ (blue) and ‡ (cyan), respectively. Neutron data have been normalized to beam monitor count and the error bars are statistical in nature and represent one standard deviation.

transition at $T_N = 7.3$ K. The primary magnetic satellite peak can be indexed with a propagation vector $k_1 = (0 \ 0 \ k_{z1})$, $k_{z1} \approx 0.23$ at 1.5 K, consistent with the recent study by Rodríguez-Velamazán et al.²⁵. To determine the magnetic structures associated with both the paraelectric phase between $T_{FE} < T < T_N$ and the ferroelectric phase below $T_{FE} = 6.8$ K, sets of nuclear and magnetic reflections were collected at 7 K and 4 K at HB3A (wave length 1.546 Å). FullProf refinement of 4 K data confirms an IC cycloidal spiral spin structure with moments mainly confined in the *ac*-plane (moment size $\sim 4.08 \mu_B$) consistent with Ref. 25. The magnetic structure at 7 K is found to be an IC collinear sinusoidal spin state with moments along the *a*-axis, with a moment size of $\sim 2.17 \mu_B$. The schematic magnetic structures at 7 K and 4 K are illustrated in Fig. 1 (b) and (c), respectively. This indicates a magnetic structure change from collinear sinusoidal to cycloidal spiral at $T_{FE} = 6.8$ K that suggests an

inverse Dzyaloshinskii-Moriya mechanism for the induced ferroelectricity as proposed in Ref. 25. However, as we will show below, the cycloid structure is strongly distorted via spin-lattice coupling.

Figure 2 shows representative L -scans along both $(0\ 0\ L)$ and $(2\ 0\ L)$ directions. The scattering intensity is plotted on a logarithmic scale. Fig. 2 (a) compares the L -scans along $(0\ 0\ L)$ measured at 1.5 K and 10 K. Besides the strong, primary IC satellite peaks, weak reflections are clearly observed at 1.5 K that can be indexed as 2nd, 3rd and 5th-order harmonics of the wave vector k_1 . Furthermore, weak commensurate peaks with a propagation vector $k_2=(0\ 0\ k_{z2})$ ($k_{z2}=0.25$) are also observed at 1.5 K. As depicted in Fig. 2 (b), both $(2\ 0\ 0.23)$ IC and $(2\ 0\ 0.25)$ commensurate peaks are observed in the L -scan along $(2\ 0\ L)$. This suggests the coexistence of commensurate and incommensurate phases at 1.5 K. The inset illustrates the temperature dependence of $(2\ 0\ 0.23)$ and $(2\ 0\ 0.25)$. Both reflections show increased intensity with decreasing temperature suggesting they are magnetic in origin. The observed spin texture (both even and odd-order harmonics associated with k_1 and coexistence of the k_2 commensurate phase) indicates the cycloidal spiral spin structure is strongly distorted since no higher-order harmonics should be observed for an ideal cycloid spiral. Furthermore, as discussed in Ref. 26, odd-order harmonics and even order harmonics are expected to be magnetic and nuclear in origin, respectively. Therefore, the observation of the 2nd-order harmonic provides direct evidence of a lattice modulation associated with the cycloid order with wave vector k_1 .

The magnetic transitions occur within a narrow temperature range at $T_N \approx 7.3$ K and $T_{FE} \approx 6.8$ K. To clarify the nature and exact transition temperature of the primary satellite and higher-order harmonic peaks, we measure both $(0\ 0\ 0.77)$ and $(0\ 0\ 2.46)$ (2nd-order harmonic) as a function of temperature by performing L scans. The obtained order parameters and peak center (indexed using k_{z1}) versus T are plotted in Fig. 3 in comparison with the specific heat data (Fig. 3 (a)). The integrated intensity was obtained by fitting the scan at each temperature to a Gaussian function with a constant background. The order parameter of $(0\ 0\ 0.77)$ (Fig. 3 (b)) shows a transition at 7.3 K corresponding to T_N and depicts no clear anomaly at T_{FE} . The order parameter of $(0\ 0\ 2.46)$ (Fig. 3 (c)) reveals that the appearance of the 2nd-order harmonic coincides with the onset of electric polarization. Fitting the order parameters to a power-law $I(T)=I_0[(T_N-T)/T_N]^{2\beta}$ yield $T_N \approx 7.34 \pm 0.02$ K and $\beta \approx 0.194 \pm 0.015$ for $(0\ 0\ 0.77)$, and $T_{FE} \approx 6.68 \pm 0.03$ K and $\beta \approx 0.245 \pm 0.002$ for $(0\ 0\ 2.46)$, respectively. The fitting results are plotted in Fig. 3 (b) and (c) as red solid curves. The fitting was performed over the temperature ranges $2\text{ K} < T < T_N$ and $2\text{ K} < T < T_{FE}$, respectively. These critical exponent β values are much smaller than the theoretical value of 0.36 predicted for a three-dimensional Heisenberg antiferromagnet (de Jongh and Miedema 1974). This suggests a lower magnetic dimen-

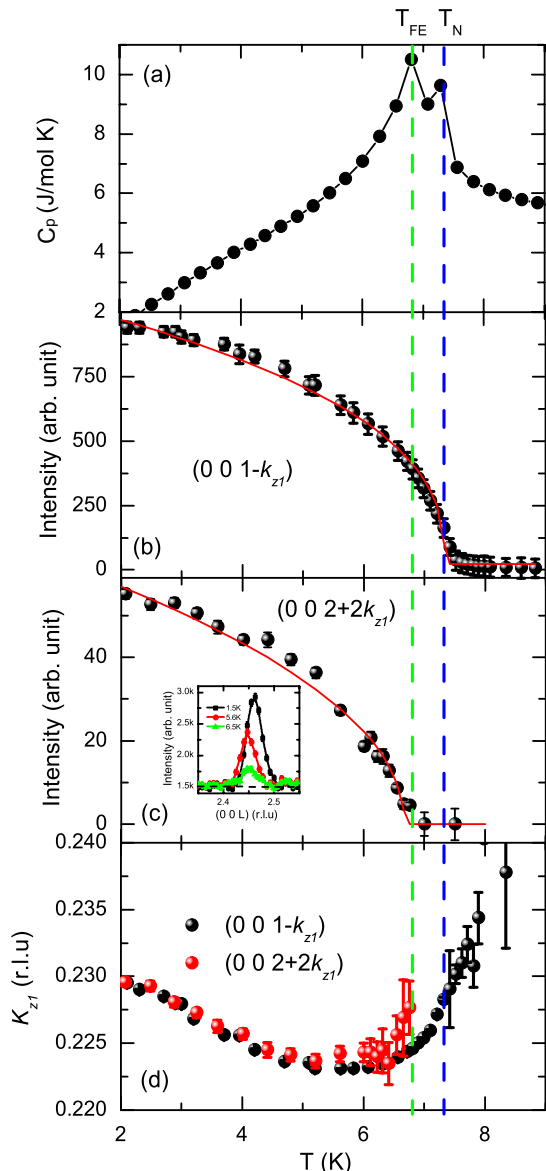


FIG. 3. (Color online) Temperature dependence of (a) the specific heat, (b) integrated intensity of the $(0\ 0\ 0.77)$ magnetic peak, and (c) integrated intensity of the $(0\ 0\ 2.46)$ 2nd-order harmonic peak. The inset in (c) shows L scans of $(0\ 0\ 2.46)$ at selected temperatures. The solid lines in (b) and (c) are fits of the order-parameter data to the power law as described in the text. (d) Temperature dependence of IC propagation vector k_{z1} determined from $(0\ 0\ 1-k_{z1})$, and $(0\ 0\ 2+2k_{z1})$. The error bar in (d) represents statistical error from the fitting, not the systematic error.

sionality of $(\text{ND}_4)_2\text{FeCl}_5 \cdot \text{D}_2\text{O}$ as proposed in Ref. 21. Temperature dependence of the IC propagation vector k_{z1} , determined by fitting the L -scans of $(0\ 0\ 0.77)$ and $(0\ 0\ 2.46)$, is plotted in Fig. 3 (d). Good agreement is obtained between $2\text{ K} < T < 6\text{ K}$, the discrepancy above 6 K can be attributed to the significant broadening of both reflections near T_{FE} and T_N . The wave vector $(0\ 0\ k_{z1})$ continues to vary with decreasing temperature through-

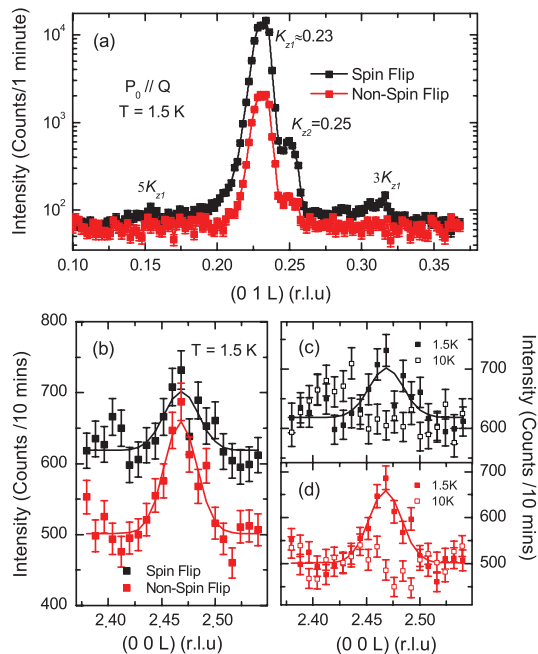


FIG. 4. (Color online) Polarized neutron data measured in the horizontal field configuration, $P_0 \parallel Q$. (a) L-scan along $[0\ 1\ L]$ measured at 1.5 K comparing the spin-flip (SF, $-+$) and non-spin-flip (NSF, $++$) scatterings with the intensity plotted on a logarithmic scale. (b) Comparison of the 1.5 K SF and NSF data suggests the hybrid nature of the $(0\ 0\ 2.46)$ 2nd-order harmonic peak. Comparison of 1.5 K and 10 K data of $(0\ 0\ 2.46)$ from (c) SF channel and (d) NSF channel, respectively.

out the ferroelectric phase and it shows no evidence of an incommensurate-commensurate (IC-C) lock-in transition down to 1.5 K.

To clarify the origin of the higher-order harmonics and k_2 -type commensurate peaks, a polarized neutron diffraction experiment was carried out using the HB1 polarized triple-axis spectrometer. Fig. 4 plots the polarized data analyzed using the method discussed in Ref. 27–29. The magnetic origin of the commensurate peak and the odd-order harmonics associated with the cycloid order is verified by the stronger scattering observed in the spin-flip (SF, $-+$) channel in Fig. 4 (a). The remaining scattering in the non-spin-flip (NSF, $++$) channel can be attributed to finite instrumental flipping ratio which is estimated to be $\sim 1/10$ by comparing the integrated intensity of SF and NSF data of the $(0\ 0\ 2)$ nuclear peak. Fig. 4 (b) compares the SF and NSF data of $(0\ 0\ 2.46)$ measured at 1.5 K. Stronger scattering intensity is detected in the NSF channel indicating the 2nd-order harmonic is dominated by nuclear scattering contribution. Weak scattering is also observed in the SF channel. The integrated intensity ratio between NSF and SF is ~ 1.8 , much smaller than the ratio of ~ 10 obtained for the nearby $(0\ 0\ 2)$ nuclear peak, suggesting a hybrid nature displaying both nuclear and magnetic characters. Fig. 4 (c) and (d) compares 1.5 K and 10 K data measured with SF and

NSF configurations, respectively. In both cases, the $(0\ 0\ 2.46)$ peak vanishes at 10 K in good agreement with the order parameter results measured with unpolarized neutrons.

The spin texture (in the form of higher-order harmonics) observed in $(\text{ND}_4)_2\text{FeCl}_5 \cdot \text{D}_2\text{O}$ is strikingly similar to that of TbMnO_3 , a well studied type-II multiferroic system^{3–9}. Three transitions are observed in TbMnO_3 at 41 K, 27 K, and 7 K³. The first one at 41 K is associated with the IC magnetic LRO transition of Mn^{3+} , and the third one at 7 K is due to the ordering of Tb^{3+} moments, typical for rare-earth compounds. The second transition at 27 K is particularly interesting and is accompanied by a dielectric anomaly and electric polarization. It has been clarified by a neutron diffraction study⁸ that this 27 K transition is associated with a magnetic structure change from an IC sinusoidally modulated collinear magnetic structure to an IC noncollinear spiral. Strong odd-order harmonics are observed indicating the spiral spin configuration is strongly distorted. In particular, the observation of a 2nd-order harmonic associated with chiral wave vector³ ignited a debate of the FE mechanism between the “pure electronic” model by Katsura, Nagaosa, and Balatsky³⁰ that suggests the electric polarization can be induced without the involvement of lattice degrees of freedom, and the “ion displacement” model that suggests a lattice distortion via spin-orbit coupling is essential for the FE polarization^{4–7}. Resonant x -ray diffraction study⁹ reveals the melting of the chiral order associated with the onset of the electric polarization at 27 K, in which the 2nd-order harmonic is unambiguously detected with an order parameter behaving similarly to what we observed in $(\text{ND}_4)_2\text{FeCl}_5 \cdot \text{D}_2\text{O}$. The intensity of the 2nd-order harmonic increases sharply at 27 K coinciding with the onset of the ferroelectricity. These experimental results combined with theory^{4–7} have classified TbMnO_3 as a prototypical material in which a cycloidal-spin structure generates an electric polarization via the spin-orbit interaction.

Comparing our results to TbMnO_3 , it is quite remarkable that almost identical behavior (spin texture) is observed in a molecular compound like $(\text{ND}_4)_2\text{FeCl}_5 \cdot \text{D}_2\text{O}$ in which the orbital angular momentum of Fe^{3+} is expected to be completely quenched. Both even and odd-order harmonics are observed. Similarly, the magnetic structure of $(\text{ND}_4)_2\text{FeCl}_5 \cdot \text{D}_2\text{O}$ changes from IC collinear sinusoidal to IC cycloidal-spiral at T_{FE} without an IC-C lock-in. The material is paraelectric between $T_{FE} < T < T_N$ and ferroelectricity only sets in below T_{FE} , where the 2nd-order harmonic appears indicating lattice distortion resulting from spin-lattice coupling. Hence, our neutron diffraction study provides unambiguous evidence that spin-lattice coupling plays a key role in its FE mechanism. Moreover, the observed coexistence of incommensurate and commensurate phases adds additional complexity in this material compared with TbMnO_3 . A preliminary inelastic neutron scattering study suggests they are both energetically favorable and the compe-

tion between these two phases is responsible for the rich magnetic field versus temperature phase diagram of $(\text{ND}_4)_2\text{FeCl}_5\cdot\text{D}_2\text{O}$ ³¹.

In summary, our neutron diffraction study on $(\text{ND}_4)_2\text{FeCl}_5\cdot\text{D}_2\text{O}$ reveals that the appearance of ferroelectricity in this molecular magnet is mediated by spin-lattice coupling. We find remarkable similarities with TbMnO_3 . Extensive experimental^{3,9} and theoretical studies⁴⁻⁷ indicate that the subtle distorted spin texture observed in TbMnO_3 plays a critical role in the FE mechanism for this prototypical system. Our study suggests $(\text{ND}_4)_2\text{FeCl}_5\cdot\text{D}_2\text{O}$ is a rare molecular analogue to TbMnO_3 . Although the incorporation of NH_4 has been used as a strategy to search for new multiferroics, however, to our knowledge only type-I multiferroics have been discovered through this approach so far¹⁷⁻¹⁹. The

spin-lattice coupling mediated FE mechanism revealed in this system certainly opens an avenue for searching new multiferroics and calls for more thorough theoretical investigations.

I. ACKNOWLEDGEMENT

The research work at ORNLs High Flux Isotope Reactor and Spallation Neutron Source was sponsored by the Scientific User Facilities Division, Office of Basic Energy Sciences, US Department of Energy. JQY, BCS and RSF were supported by the Department of Energy, Office of Science, Basic Energy Sciences, Materials Sciences and Engineering Division.

-
- * wt6@ornl.gov
- ¹ Sang-wook Cheong and Maxim Mostovoy, *Nat. Mater* (London), **6**, 13-20 (2007).
 - ² Daniel Khomskii, *Physics* **2**, 20 (2009).
 - ³ T. Kimura, T. Goto, H. Shintani, K. Ishizaka, T. Arima, and Y. Tokura, *Nature* (London) **426**, 55 (2003).
 - ⁴ I. A. Sergienko and E. Dagotto, *Phys. Rev. B* **73**, 094434 (2006).
 - ⁵ H. J. Xiang, S.-H. Wei, M.-H. Whangbo, and J. L. F. Da Silva, *Phys. Rev. Lett.* **101**, 037209 (2008).
 - ⁶ Andrei Malashevich and David Vanderbilt, *Phys. Rev. Lett.* **101**, 037210 (2008).
 - ⁷ I. V. Solovyev, *Phys. Rev. B* **83**, 054404 (2011).
 - ⁸ M. Kenzelmann, A. B. Harris, S. Jonas, C. Broholm, J. Schefer, S. B. Kim, C. L. Zhang, S.-W. Cheong, O. P. Vajk, and J.W. Lynn, *Phys. Rev. Lett.* **95**, 087206 (2005).
 - ⁹ S. W. Lovesey, V. Scagnoli, M. Garganourakis, S. M. Koohpayeh, C Detlefs and U Staub, *J. Phys.: Condens. Matter* **25**, 362202 (2013).
 - ¹⁰ K. Taniguchi *et al.*, *Phys. Rev. Lett.* **97**, 097203 (2006).
 - ¹¹ G. Lawes *et al.*, *Phys. Rev. Lett.* **95**, 087205 (2005).
 - ¹² R. Vilarreal, G. Quirion, M. L. Plumer, M. Poirier, T. Usui, and T. Kimura, *Phys. Rev. Lett.* **109**, 167206 (2012).
 - ¹³ H. J. Xiang and M.-H. Whangbo, *Phys. Rev. Lett.* **99**, 257203 (2007).
 - ¹⁴ Y. J. Choi, H. T. Yi, S. Lee, Q. Huang, K. Kiryukhin, and S.-W. Cheongs, *Phys. Rev. Lett.* **100**, 047601 (2008).
 - ¹⁵ Omar M. Yaghi *et al.* *Nature* **423**, 705 (2003).
 - ¹⁶ A. H. Rama Rao, M. R. Srinivasan, H. L. Bhat and P. S. Narayana, *Ferroelectrics* **21** 433(1978).
 - ¹⁷ Raghavendra Samantaray, Ronald J. Clark, Eun S. Choi, and Naresh S. Dalal, *J. Am. Chem. Soc.* **134**, 15953-15962 (2012).
 - ¹⁸ Guan-Cheng Xu *et al.* *J. Am. Chem. Soc.* **133**, 14948-14951 (2011).
 - ¹⁹ R. Samantaray *et al.* *J. Am. Chem. Soc.* 2011, **133**, 3792-3795 (2011).
 - ²⁰ Carlin R L *et al.*, *J. Am. Chem. Soc.* **99** 7728 (1977).
 - ²¹ J. N. McElearney, and S. Merchant, *Inorganic Chemistry*, Vol. **17**, No. 5,(1978).
 - ²² M Gabás, F Palacio, J Rodriguez-Carvajal, and D Visser, *J. Phys.: Condens. Matter* **7**, 4725-4738 (1995).
 - ²³ Javier Campo, Javier Luzón, Fernando Palacio, Garry J. McIntyre, Angel Millán, and Andrew R. Wildes, *Phys. Rev. B* **78**, 054415 (2008).
 - ²⁴ M Ackermann, D Brüning, T Lorenz, P Becker, and L Bohatý, *New Journal of Physics* **15**, 123001 (2013).
 - ²⁵ Jose Alberto Rodriguez-Velamazán, Oscar Fabelo, Angel Millan, Javier Campo, Roger D. Johnson, and Laurent Chapon, *Scientific Reports*, 5:14475, DOI: 10.1038/srep14475.
 - ²⁶ K. Hirai, *J. Phys. Soc. Jpn.* **66**, 560 (1997).
 - ²⁷ R. M. Moon, T. Kiste, and W. C. Koehler, *Phys. Rev.* **181**, 920 (1969).
 - ²⁸ Q. Huang, P. Karen, V. L. Karen, A. Kjekshus, J. W. Lynn, A. D. Mighell, N. Rosov, and A. Santoro, *Phys. Rev. B* **45**, 9611 (1992).
 - ²⁹ J. W. Lynn, N. Rosov, and G. Fish, *J. Appl. Phys.* **73**, 5369 (1993).
 - ³⁰ H. Katsura, N. Nagaosa, and A. V. Balatsky, *Phys. Rev. Lett.* **95**, 057205 (2005).
 - ³¹ W. Tian *et al.* unpublished.